Teleportation of entanglement over 143 km

Thomas Herbst[a,b,1], Thomas Scheidl[a,b], Matthias Fink[a,b], Johannes Handsteiner[a,b], Bernhard Wittmann[a,b], Rupert Ursin[a,b], and Anton Zeilinger[a,b,1]

[a]Vienna Center for Quantum Science and Technology, Faculty of Physics, University of Vienna, A-1090 Vienna, Austria; and [b]Institute for Quantum Optics and Quantum Information, Austrian Academy of Sciences, A-1090 Vienna, Austria

As a direct consequence of the no-cloning theorem, the deterministic amplification as in classical communication is impossible for unknown quantum states. This calls for more advanced techniques in a future global quantum network, e.g., for cloud quantum computing. A unique solution is the teleportation of an entangled state, i.e., entanglement swapping, representing the central resource to relay entanglement between distant nodes. Together with entanglement purification and a quantum memory it constitutes a so-called quantum repeater. Since the aforementioned building blocks have been individually demonstrated in laboratory setups only, the applicability of the required technology in real-world scenarios remained to be proven. Here we present a free-space entanglement-swapping experiment between the Canary Islands of La Palma and Tenerife, verifying the presence of quantum entanglement between two previously independent photons separated by 143 km. We obtained an expectation value for the entanglement-witness operator, more than 6 SDs beyond the classical limit. By consecutive generation of the two required photon pairs and space-like separation of the relevant measurement events, we also showed the feasibility of the swapping protocol in a long-distance scenario, where the independence of the nodes is highly demanded. Because our results already allow for efficient implementation of entanglement purification, we anticipate our research to lay the ground for a fully fledged quantum repeater over a realistic high-loss and even turbulent quantum channel.

quantum | repeater | entanglement | teleportation | swapping

Because an unknown single quantum state cannot be cloned or amplified without destroying its essential quantum feature (1), the quantum repeater (2–4) is the main device for faithful entanglement distribution over long distances. The idea is to decompose the total distance into shorter elementary links, over which entanglement is shared, purified, and eventually stored in quantum memories. Once all of the nodes are set the entangled states can be retrieved on demand. Finally the entanglement is swapped between adjacent nodes and faithfully extended over the whole distance. Entanglement purification (5–7) and quantum memories (4, 8) serve solely to enhance the efficiency and the fidelity of the protocol, both of which are limited due to imperfection of the sources of entangled particles, of the involved quantum operations, and of the interconnecting quantum channels. Entanglement swapping (9–17) however provides the underlying nonclassical correlations and constitutes the fundamental process required for the implementation of a quantum repeater. Here we show that we were able to provide this resource via a realistic 143-km long-distance free-space (elementary) link under harsh atmospheric conditions, representing to our knowledge the largest geographical separation for this protocol to date. Furthermore, the simultaneous creation of two randomly generated photon pairs drastically reduces the signal-to-noise ratio, leading to technological requirements on the verge of practicability. Nonetheless, we ensured space-like separation of the remote measurement events, which is important for certain protocols, e.g., quantum key distribution (18, 19).

The entanglement swapping protocol is realized via the generation of two entangled pairs, photons "0" and "1" and photons "2" and "3," for example the maximally entangled singlet states

$$|\Psi^-\rangle_{01} = 1/\sqrt{2}\big(|H\rangle_0|V\rangle_1 - |V\rangle_0|H\rangle_1\big)$$

$$|\Psi^-\rangle_{23} = 1/\sqrt{2}\big(|H\rangle_2|V\rangle_3 - |V\rangle_2|H\rangle_3\big), \qquad [1]$$

where $|H\rangle$ and $|V\rangle$ denote the horizontal and vertical polarization states, respectively. The product state $|\Psi\rangle_{0123} = |\Psi^-\rangle_{01} \otimes |\Psi^-\rangle_{23}$ may be written as

$$|\Psi^-\rangle_{0123} = 1/2\big(|\Psi^+\rangle_{03} \otimes |\Psi^+\rangle_{12} - |\Psi^-\rangle_{03} \otimes |\Psi^-\rangle_{12}$$
$$- |\Phi^+\rangle_{03} \otimes |\Phi^+\rangle_{12} + |\Phi^-\rangle_{03} \otimes |\Phi^-\rangle_{12}\big). \qquad [2]$$

Therefore, a so-called Bell-state measurement (BSM) between photons "1" and "2" results randomly in one of the four maximally entangled Bell states $|\Psi^\pm\rangle_{12} = 1/\sqrt{2}\,(|H\rangle_1|V\rangle_2 \pm |V\rangle_1|H\rangle_2)$ and $|\Phi^\pm\rangle_{12} = 1/\sqrt{2}\,(|H\rangle_1|H\rangle_2 \pm |V\rangle_1|V\rangle_2)$ with an equal probability of 1/4. By that measurement, photons "0" and "3" are projected into the same entangled state as photons "1" and "2." Thus, the entanglement is swapped from photons "0-1" and "2-3" to the photons "1-2" and "0-3." This procedure may also be seen as teleportation of the state of photon "1" onto photon "3" or photon "2" onto photon "0." Although the implementation of this protocol, solely based on linear optics, allows distinguishing between two out of four Bell states only (20), it provides a maximal fidelity of 1 in the successful cases.

Significance

Teleportation of an entangled state, also known as entanglement swapping, plays a vital role in the vision of a global quantum internet, providing unconditionally secure communication, blind cloud computing, and an exponential speedup in distributed quantum computation. In contrast to the teleportation of a single quantum state from one qubit to another, entanglement swapping generates entanglement between two independent qubits that have never interacted in the past. Therefore this protocol represents a key resource for numerous quantum-information applications that has been implemented in many different systems to date. We experimentally demonstrated entanglement swapping over 143 km between the Canary Islands of La Palma and Tenerife, proving the feasibility of this protocol to be implemented in a future global scenario.
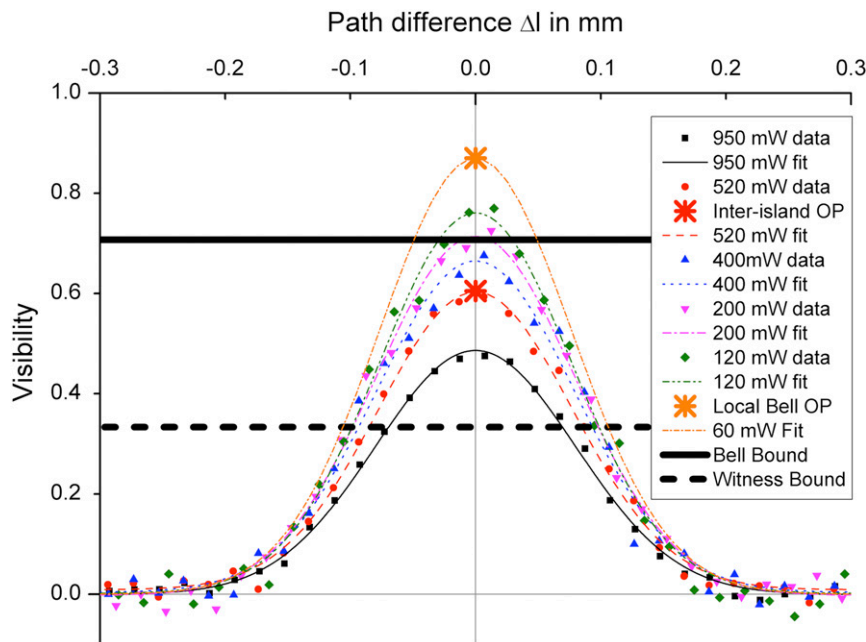
Experiment

Here we report successful entanglement swapping in an experiment performed on the Canary Islands, using a 143-km horizontal free-space link between the Jacobus Kapteyn Telescope (JKT) building of the Isaac Newton Group of Telescopes (ING) on La Palma and the Optical Ground Station (OGS) of the European Space Agency (ESA) on Tenerife. Both buildings are located at an elevation of 2,400 m above sea level. The JKT served as the base station for the production of the two entangled photon pairs, for the BSM between photons "1" and "2" and for the polarization detection of photon "0" at Alice. The transmitter telescope, sending photon "3" to the receiving station on Tenerife, was installed on the rooftop of the JKT building. At the receiver the photons were collected by the 1-m-diameter OGS reflector telescope and guided through the optical Coudé path to the setup for polarization analysis and the final measurement by Bob.

In our experimental setup (Fig. 1) a mode-locked femtosecond pulsed Ti:Saph laser emitted light with a central wavelength of 808 nm at a repetition rate of 80 MHz. Those near-infrared pulses were then frequency doubled to a central wavelength of 404 nm using second-harmonic generation in a type-I nonlinear β-barium borate (BBO) crystal. The individual polarization-entangled photon pairs used in the protocol were generated via spontaneous parametric down-conversion (SPDC) in two subsequent type-II phase-matched BBOs (21) and coupled into single-mode (SM) optical fibers for spatial mode selection. Eliminating the spectral distinguishability, which is inherent to pulsed SPDC schemes, optimized the quality of entanglement. We therefore decoupled the photon pairs' spectral degree of freedom from the polarization degree of freedom using the scheme as outlined in refs. 22–24. The first SPDC source provided the entangled state $|\Psi^-\rangle_{23}$, with photon "2" as one input photon for the BSM and photon "3" being guided through a 50-m-long SM fiber to the transmitter telescope. The subsequent SPDC source prepared the state $|\Psi^-\rangle_{01}$, where photon "1" was the second input photon for the BSM. Photon "0" was locally delayed in a 100-m fiber (∼500 ns) and subsequently measured by Alice, thus ensuring space-like separation between Alice's and Bob's measurement events (19).

In La Palma, the BSM was implemented using a tunable fiber beam splitter (FBS) set to a 50:50 splitting ratio. Whereas the spatial overlap of photons "1" and "2" is inherent to the FBS, a perfect temporal overlap is accomplished in the minimum of the Hong–Ou–Mandel (25) interference dip. The latter was achieved by adjusting the optical path length for photon "2" by linearly moving the SM fiber coupler in the first SPDC source. Both

Fig. 1. Entanglement swapping over a 143-km free-space channel between the Canary Islands of La Palma and Tenerife. Both SPDC sources, the BSM module and Alice, were situated on La Palma and Bob on Tenerife. The two SPDC sources generated the entangled photon pairs "0-1" and "2-3." Photons "1" and "2" (photons are indicated by black numbers on red circles) were subjected to a BSM. A 100-m fiber delayed photon "0" with respect to photon "3," such that Alice's and Bob's measurements were space-like separated. Revealing entanglement of photons "0" and "3" between Alice and Bob verified successful entanglement swapping. Polarization-entangled photon pairs $|\Psi^-\rangle_{01}$ and $|\Psi^-\rangle_{23}$ were generated in two identical sources via SPDC in a nonlinear BBO crystal. The photons were then coupled into SM fibers with fiber couplers. Any polarization rotation in the SM fibers was compensated for by fiber polarization controllers. Photons "1" and "2" were spectrally filtered with interference filters (IFs) with a full width at half maximum (FWHM) of 3 nm and overlapped in an FBS. A subsequent polarization-dependent measurement was performed, using a quarter-wave plate (QWP), a half-wave plate (HWP), a PBS, and four APDs (a, b, c, and d) in the BSM. Photon "3" was guided via a 50-m fiber to the transmitter (Tx) and sent to Bob in Tenerife, whereas photon "0" was delayed by a 100-m fiber before its polarization detection at Alice. The receiver (Rx) on Tenerife captured photon "3" where Bob performed his polarization-dependent measurement. Both Alice and Bob spectrally filtered their photons with IFs with 8-nm FWHM. All detection events were time stamped by TTU with a resolution of 156 ps and stored for subsequent analysis. See the text for further details.

Fig. 2. Plot of the entanglement-swapping visibility versus path-length difference for different pump powers locally measured on La Palma. The abscissa represents the relative optical path-length difference Δl in mm between photon "1" and "2" in the BSM and the ordinate represents the entanglement-swapping visibility. Black squares, red dots, blue triangles, purple upside-down triangles, and green diamonds indicate the data points of the visibilities at 950-, 520-, 400-, 200-, and 120-mW average pump power, respectively. The entanglement-witness bound and the bound for the violation of a CHSH-type Bell inequality are represented by a black dashed and a black solid line at visibilities of 1/3 and $1/\sqrt{2}$, respectively. The operating point (OP) for the local test of the CHSH inequality was chosen at a pump power of 60 mW and zero delay (orange asterisk). At this set point a visibility of 0.87 was achieved. For the entanglement-swapping experiment via the 143-km and −32-dB free-space link we tuned the setup to a visibility of 0.6 at 520-mW average pump power (red asterisk) and again perfect overlap at zero delay.

output arms of the FBS were equipped with a quarter- and a half-wave plate followed by a polarizing beam splitter (PBS) in order to project on any desired polarization measurement basis. Intrinsic polarization rotations in the SM fibers were compensated for with in-fiber polarization controllers. The avalanche photodiodes (APDs) a, b, c, and d, placed at the four outputs of the two PBSs, were connected to a home-made coincidence logic, providing the two valid outcomes of our BSM: simultaneous clicks of APDs (a and d) ∨ (b and c) or (a and b) ∨ (c and d) (where ∨ denotes the logical OR operator) indicated that photons "1" and "2" were projected onto the maximally entangled $|\Psi^-\rangle_{12}$ singlet or $|\Psi^+\rangle_{12}$ triplet Bell state, respectively. As can be seen from Eq. 2, conditioned on these BSM results, photons "0" and "3" were thus simultaneously projected onto the very same states $|\Psi^-\rangle_{03}$ and $|\Psi^+\rangle_{03}$, respectively. The projection onto the other Bell states $|\Phi^\pm\rangle_{12}$ does not result in a coincidence detection event by the BSM and thus cannot be resolved with a linear-optics scheme. Furthermore, the two valid BSM outcomes together with Alice's detection events of photon "0" (APDs e and f) were fed into a logic AND gate, providing four possible combinations. These local threefold coincidence events on La Palma as well as the remote detection events of photon "3" on Tenerife (APDs g and h) were then recorded by two separate time-tagging units (TTUs) with a temporal resolution of 156 ps. To retrieve the final fourfolds between Alice's events and those measured on Bob's side we calculated the cross-correlation between the remotely recorded individual measurement data—both synchronized to the Global Positioning System (GPS) standard time. To compensate for residual relative clock drifts between the distant TTU clocks we harnessed the temporal correlations of our entangled photon pairs. This clock synchronization (26) between consecutive 30-s measurements allowed for a coincidence-time window of down to 5 ns.

The strong average attenuation of −32 dB over the 143-km free-space quantum channel calls for high production rates of the SPDC sources to operate well above the noise level of the single-photon detectors on Tenerife. However, pumping the SPDC sources with high pump intensities reduces the achievable entanglement-swapping visibility (i.e., the average visibility of states $|\Psi^-\rangle_{03}$ and $|\Psi^+\rangle_{03}$) due to increased multipair emissions. Hence, a reasonable trade-off between count rates and this visibility was required. To find the optimal operating point, we locally characterized our setup for various pump powers of the SPDC sources (Fig. 2). The entanglement-swapping visibilities of our setup varied between 0.87 at lowest average pump power of

Table 1. Measurement results

Swapped state	$|\Psi^-\rangle_{03}$	$|\Psi^+\rangle_{03}$
$V_{H/V}$	0.618 ± 0.067	0.610 ± 0.062
$V_{P/M}$	0.607 ± 0.060	0.556 ± 0.065
$V_{R/L}$	0.624 ± 0.056	0.542 ± 0.065
$\overline{V}$	0.616 ± 0.035	0.569 ± 0.037
$W = 1/2 - (1 + 3\overline{V})/4$	-0.212 ± 0.027	-0.177 ± 0.028
Local S value	2.487 ± 0.287	2.469 ± 0.287

Numerical values of the measurement results including the individual visibilities $V_{H/M}$, $V_{P/M}$, and $V_{R/L}$ in the three mutually unbiased bases horizontal/vertical (H/V), plus/minus (P/M), and right/left (R/L) as well as the mean visibility V, the expectation value of the entanglement-witness operator W, and the locally measured S value. Over the 143-km free-space link the entanglement witness was more than 6 SDs beyond the classical bound of 0. This proved the presence of entanglement between photons "0" and "3" in the states $|\Psi^-\rangle_{03}$ and $|\Psi^+\rangle_{03}$. The violation of a CHSH-type Bell inequality was shown locally on La Palma, underlining the quality of our setup. All outcomes are given for the swapped states $|\Psi^-\rangle_{03}$ and $|\Psi^+\rangle_{03}$ with the respective SDs assuming Poissonian photon statistics.

Herbst et al.

60 mW and 0.49 at 950 mW full pump power. At lowest pump power we locally detected a twofold rate of 15,000 counts per second (cps) and a fourfold rate of about 1 cps. Full pump power yielded 240,000 cps twofolds and 370 cps fourfolds.

A traditional measure of entanglement is constituted by violation of a Clauser–Horne–Shimony–Holt (27) (CHSH)-type Bell inequality. To accomplish this, a CHSH S value above the classical bound of $S \leq 2$ needs to be experimentally obtained, being equivalent to an entanglement visibility of $1/\sqrt{2} \sim 0.71$. This was only achievable when operating at low pump powers and, given the resulting low count rates, therefore only feasible in the course of a measurement performed locally on La Palma. Nevertheless, such a local measurement serves to indicate the quality of the setup and to estimate the functionality over the long distance. We accumulated data over 8,000 s and measured the required S value for both the singlet $|\Psi^-\rangle_{03}$ and triplet $|\Psi^+\rangle_{03}$ state. In total we detected 5,647 singlet and 5,618 triplet swapping events and violated the inequality with $S_{singlet} = 2.487 \pm 0.287$ and $S_{triplet} = 2.469 \pm 0.287$ at an average pump power of 60 mW, respectively (Table 1). This result clearly proves that photons "0" and "3" were projected into an entangled state.

To reduce the accumulation time in the remote measurement scenario, we increased the average pump power to 520 mW, corresponding to a locally detected fourfold count rate of 100 cps and an average entanglement visibility of the swapped state of ∼0.60. We measured the expectation value of an entanglement-witness operator W, with $W < 0$ representing a sufficient condition for the presence of entanglement (28). Our entanglement-witness operator is given as

$$W = 1/2 - 1/4\left(1 + V_{H/V} + V_{P/M} + V_{R/L}\right), \qquad [3]$$

with $V_{H/V}$, $V_{P/M}$, $V_{R/L}$ being the correlation visibilities of state $|\Psi\rangle_{03}$ in the three mutually unbiased bases horizontal/vertical (H/V), plus/minus (P/M) and right/left (R/L), respectively. The visibility is given by $V = (CC_{max} - CC_{min})/(CC_{max} + CC_{min})$ with

the max (min) coincidence counts CC_{max} (CC_{min}). Inserting the measured visibilities into Eq. **3** yields a negative expectation value for the entanglement-witness operator $W_{singlet} = -0.212 \pm 0.027$ and $W_{triplet} = -0.177 \pm 0.028$ with statistical significances of 7.99 and 6.37 SDs, respectively (assuming Poissonian photon statistics). Hence, we unambiguously demonstrated that the experimentally obtained states between photon "0" and "3" became entangled over 143 km (Table 1). These results were obtained from subsequent 30-s data files, accumulated over a measurement time of 271 min during four consecutive nights. In total, 506 and 492 entanglement-swapping events have been recorded for the singlet and triplet state, respectively.

Our data demonstrate successful entanglement swapping via a long-distance free-space link under the influence of highly demanding environmental conditions, in fact more challenging than expected for a satellite-to-ground link. This proves the feasibility of a crucial element for realizing a quantum repeater in a future space- and ground-based worldwide quantum internet (29, 30) and for distributed quantum computation (31–34). In particular, in a quantum repeater scheme assuming perfect quantum memories, a single step of the purification method realized in ref. 7 would increase our obtained visibilities beyond the bound for the violation of a CHSH-type Bell inequality even in the remote scenario. Together with a reliable quantum memory, our results set the benchmark for an efficient quantum repeater at the heart of a global quantum-communication network.

1. Wootters WK, Zurek WH (1982) A single quantum cannot be cloned. *Nature* 299(5886):802–803.
2. Briegel HJ, Dür W, Cirac J, Zoller P (1998) Quantum repeaters: The role of imperfect local operations in quantum communication. *Phys Rev Lett* 81(26):5932–5935.
3. Duan LM, Lukin MD, Cirac JI, Zoller P (2001) Long-distance quantum communication with atomic ensembles and linear optics. *Nature* 414(6862):413–418.
4. Gisin N, Thew R (2007) Quantum communication. *Nat Photonics* 1(3):165–171.
5. Bennett CH, et al. (1996) Purification of noisy entanglement and faithful teleportation via noisy channels. *Phys Rev Lett* 76(5):722–725.
6. Pan J-W, Simon C, Brukner C, Zeilinger A (2001) Entanglement purification for quantum communication. *Nature* 410(6832):1067–1070.
7. Pan J-W, Gasparoni S, Ursin R, Weihs G, Zeilinger A (2003) Experimental entanglement purification of arbitrary unknown states. *Nature* 423(6938):417–422.
8. Clausen C, et al. (2011) Quantum storage of photonic entanglement in a crystal. *Nature* 469(7331):508–511.
9. Zukowski M, Zeilinger A, Horne MA, Ekert AK (1993) "Event-ready-detectors" Bell experiment via entanglement swapping. *Phys Rev Lett* 71(26):4287–4290.
10. Bose S, Vedral V, Knight PL (1998) Multiparticle generalization of entanglement swapping. *Phys Rev A* 57(2):822–829.
11. Pan J-W, Bouwmeester D, Weinfurter H, Zeilinger A (1998) Experimental entanglement swapping: Entangling photons that never interacted. *Phys Rev Lett* 80(18):3891–3894.
12. Jennewein T, Weihs G, Pan J-W, Zeilinger A (2002) Experimental nonlocality proof of quantum teleportation and entanglement swapping. *Phys Rev Lett* 88(1):017903-1–017903-4.
13. Halder M, et al. (2007) Entangling independent photons by time measurement. *Nat Phys* 3(10):692–695.
14. Yuan Z-S, et al. (2008) Experimental demonstration of a BDCZ quantum repeater node. *Nature* 454(7208):1098–1101.
15. Kaltenbaek R, Prevedel R, Aspelmeyer M, Zeilinger A (2009) High-fidelity entanglement swapping with fully independent sources. *Phys Rev Lett* 79(4):040302-1–040302-4.
16. Ma X-S, et al. (2012) Experimental delayed-choice entanglement swapping. *Nat Phys* 8(6):479–484.
17. Hofmann J, et al. (2012) Heralded entanglement between widely separated atoms. *Science* 337(6090):72–75.
18. Ekert AK (1991) Quantum cryptography based on Bell's theorem. *Phys Rev Lett* 67(6):661–663.
19. Scheidl T, et al. (2010) Violation of local realism with freedom of choice. *Proc Natl Acad Sci USA* 107(46):19708–19713.
20. Calsamiglia J, Lütkenhaus N (2001) Maximum efficiency for a linear-optical Bell-state analyzer. *Appl Phys B* 72(1):67–71.
21. Kwiat PG, et al. (1995) New high-intensity source of polarization-entangled photon pairs. *Phys Rev Lett* 75(24):4337–4341.
22. Kim Y-H, Grice WP (2002) Generation of pulsed polarization-entangled two-photon state via temporal and spectral engineering. *J Mod Opt* 49(14-15):2309–2323.
23. Kim Y-H, Kulik SP, Chekhova MV, Grice WP, Shih Y (2003) Experimental entanglement concentration and universal Bell-state synthesizer. *Phys Rev A* 67(1):010301-1–010301-4.
24. Poh H, Lim J, Marcikic I, Lamas-Linares A, Kurtsiefer C (2009) Eliminating spectral distinguishability in ultrafast spontaneous parametric down-conversion. *Phys Rev Lett* 80(4):043815-1–043815-6.
25. Hong CK, Ou ZY, Mandel L (1987) Measurement of subpicosecond time intervals between two photons by interference. *Phys Rev Lett* 59(18):2044–2046.
26. Ma X-S, et al. (2012) Quantum teleportation over 143 kilometres using active feed-forward. *Nature* 489(7415):269–273.
27. Clauser JF, Horne MA, Shimony A, Holt RA (1969) Proposed experiment to test local hidden-variable theories. *Phys Rev Lett* 23(15):880–884.
28. Gühne O, Tóth G (2009) Entanglement detection. *Phys Rep* 474(1-6):1–75.
29. Kimble HJ (2008) The quantum internet. *Nature* 453(7198):1023–1030.
30. Zhang J, et al. (2013) Quantum internet using code division multiple access. *Sci Rep* 3:2211.
31. Cirac JI, Ekert AK, Huelga SF, Macchiavello C (1999) Distributed quantum computation over noisy channels. *Phys Rev A* 59(6):4249–4254.
32. Nielsen MA, Chuang IL (2000) *Quantum Computation and Quantum Information* (Cambridge Univ Press, New York).
33. Buluta I, Ashhab S, Nori F (2011) Natural and artificial atoms for quantum computation. *Rep Prog Phys* 74(10):104401–104416.
34. Barz S, et al. (2012) Demonstration of blind quantum computing. *Science* 335(6066):303–308.

PHYSICS